

Uniaxial hybridization in the quasi-one-dimensional Kondo lattice CeCo_2Ga_8

P. Zheng^{1,2,*}, Cuixiang Wang^{1,2}, Yuanji Xu^{1,2}, L. Wang^{1,2}, W. Wu^{1,2}, Y. G. Shi^{1,2,3}, Yi-feng Yang^{1,2,3,†} and J. L. Luo^{1,2,3}

¹Beijing National Laboratory for Condensed Matter Physics and Institute of Physics, Chinese Academy of Sciences, Beijing 100190, China

²School of Physical Sciences, University of Chinese Academy of Sciences, Beijing 100190, China

³Songshan Lake Materials Laboratory, Dongguan, Guangdong 523808, China



(Received 20 August 2021; revised 1 December 2021; accepted 3 January 2022; published 7 January 2022)

We report the electron dynamics of the recently discovered quasi-one-dimensional Kondo lattice compound CeCo_2Ga_8 by optical spectra measurements using polarized light. For an electric field along the c axis, the high-temperature Drude-like peak is found to split into two distinct components below the coherence temperature T^* , including a narrower Drude-like peak at low frequencies characterizing the emergent heavy electron state with a large mass enhancement, and a midinfrared Lorentz-like peak originating from interband transitions across the hybridization gap. The splitting is, however, absent for an electric field along the perpendicular directions, suggesting that the hybridization only occurs along the c axis, although the high-temperature optical spectra from the background conduction electrons are isotropic. Our observations are in agreement with the resistivity data that show a broad maximum at around 20 K only along the c axis but which keep increasing with a lowering temperature below 50 K along the ab plane. Our work confirms the quasi-one-dimensional nature of the heavy electron physics in CeCo_2Ga_8 and establishes a direct correspondence between the bulk transport properties and microscopic electronic structures. It also pushes the previous observation of anisotropic coherence temperature in many heavy fermion compounds to an extreme situation and reveals the importance of intersite magnetic correlations beyond the local Kondo picture.

DOI: [10.1103/PhysRevB.105.035112](https://doi.org/10.1103/PhysRevB.105.035112)

Underlying the rich variety of correlated phenomena such as the quantum criticality and unconventional superconductivity in heavy fermion materials [1–5] is the special charge dynamics of their heavy electron normal state. The latter is associated with the localized-to-itinerant transition of f electrons and emerges below a characteristic temperature T^* often marked by a broad maximum in the resistivity measurements [6]. What has not been well established is how these bulk properties might be associated or determined by microscopic electronic structures such as the hybridization between f and conduction bands. The widely used dynamical mean-field theory typically predicts a local Kondo picture for the hybridization [7].

CeCo_2Ga_8 is a recently synthesized Kondo lattice compound, showing a quantum critical point at ambient pressure without tuning [8]. Bulk susceptibility measurements revealed large anisotropy and first-principles calculations suggest quasi-one-dimensional (1D) heavy electron Fermi surfaces [8,9]. Interestingly, unlike the resistivity which shows a linear temperature dependence below 2 K, the specific heat coefficient becomes saturated at low temperatures [8]. This disparate behavior resembles that observed in Ge-doped YbRh_2Si_2 [2,10] and was considered to signal the unconventional nature of its quantum criticality whose nature has been an issue of intensive debates during the past decade [10].

In YbRh_2Si_2 , some argue that such a disparity might be associated with a dimensional crossover [11]. Dimensionality seems indeed important for heavy fermion physics. A ferromagnetic quantum critical point has recently been observed in quasi-1D Kondo lattice systems $\text{YbNi}_4(\text{P}_{0.91}\text{As}_{0.08})_2$ and CeRh_6Ge_4 [12,13], in contrast to the usual first-order ferromagnetic transition. It is therefore a question if low dimensionality might also play a role in CeCo_2Ga_8 .

In this paper, we report detailed optical conductivity measurements in a single crystal of CeCo_2Ga_8 along different electric field directions. We find that the hybridization gap only opens along the c axis below the coherence temperature but is absent in the perpendicular directions down to our lowest measured temperature. Although we cannot reach a region with linear-in- T resistivity, our data provide unambiguous evidence for the quasi-1D property of its heavy electron state that might be useful for future clarifications of its low-temperature quantum criticality. The uniaxial hybridization property also agrees well with the anisotropy of the resistivity data, suggesting a close relation between microscopic electronic structures and macroscopic bulk properties. Our observation establishes CeCo_2Ga_8 as a true quasi-1D Kondo lattice and implies the importance of intersite magnetic interactions on the emergence of heavy electrons.

Single crystals of CeCo_2Ga_8 were grown using the self-flux method [8]. We have selected a natural as-grown surface of the single crystal of about 4.5 mm in length along the c axis for our study. The Ce ions are located at the center of the pentagons piled up by five CoGa_9 cages and which form parallel spin chains along the c axis [8]. The interchain

*pzheng@iphy.ac.cn

†yifeng@iphy.ac.cn

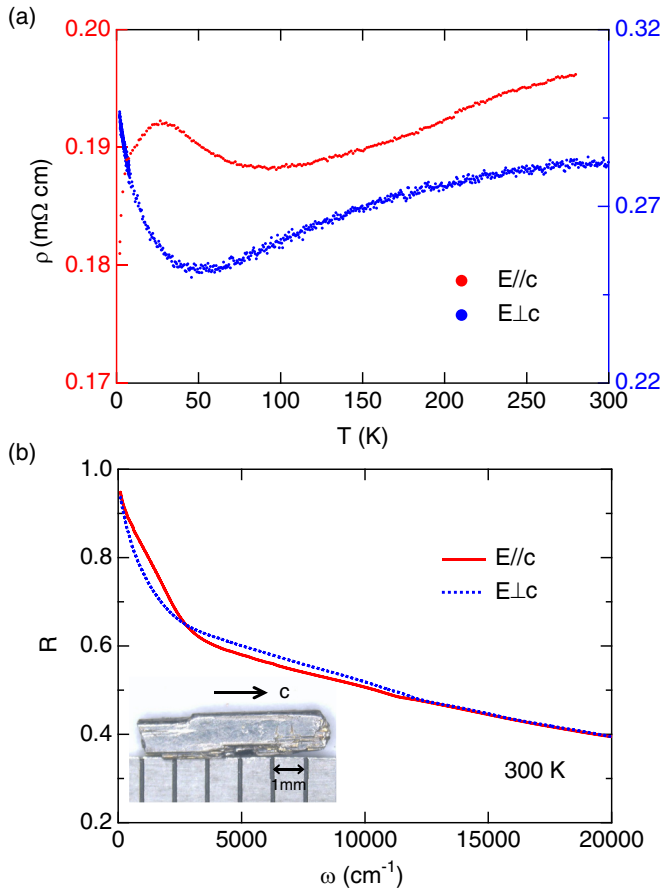


FIG. 1. (a) Comparison of the resistivity as a function of temperature along and perpendicular to the c axis. (b) Reflectivity spectra $R(\omega)$ along both directions at 300 K. The inset shows the sample.

distance between Ce atoms is about 6.5–7.5 Å, much larger than their intrachain distance of about 4.05 Å, supporting the quasi-1D Kondo lattice structure of CeCo_2Ga_8 . The dc resistivity was measured with the standard four-probe method in a Quantum Design physical property measurement system (PPMS) and shown in Fig. 1(a) for both $E \parallel c$ and $E \perp c$. The c -axis resistivity agrees qualitatively with previous data [8], with a broad maximum marking the crossover from incoherent Kondo scattering to a coherent heavy electron state. By contrast, the perpendicular resistivity keeps increasing with lowering temperature below 50 K all the way down to our lowest measured temperature of 2 K [9]. We ascribe this to the incoherent Kondo scattering within the ab plane, even though the f electrons are supposed to be itinerant along the c axis at low temperatures. It thus seems that the localized-to-itinerant transition occurs only along the c axis and the f electrons exhibit distinct characters along different directions.

To establish this highly anisotropic electronic behavior on a microscopic level, we measured the frequency-dependent reflectivity $R(\omega)$ between 80 and 25 000 cm^{-1} at temperatures from 300 K down to 6 K. The measurements were performed on a Bruker Vertex 80v spectrometer with a He flowing cryostat using a polarized light along and perpendicular to the c axis, respectively. An *in situ* overcoating technique has been used for the reflectance measurement. Surprisingly,

the spectra merge together and seem quite isotropic above 12 000 cm^{-1} , as shown in Fig. 1(b). But at low temperatures and in the far-infrared and midinfrared regions, we observed clear anisotropy. To see this, we applied the standard Hagen-Rubens relation for metal, $R(\omega) = 1 - A\sqrt{\omega}$, where A is a fitting parameter, for the low-frequency extrapolation of the reflectivity. At high frequencies, the reflectivity curve was extrapolated to 800 000 cm^{-1} with a function of $\omega^{-0.5}$, above which a function of ω^{-4} was used following Ref. [14]. The optical conductivity was then derived using the Kramers-Kronig (KK) transformation. We have also tried the constant extrapolation for the low-frequency $R(\omega)$ and found the resulting optical conductivity to be robust in the measured frequency range above 80 cm^{-1} .

We first focus on the c -axis reflectivity spectra $R(\omega)$ plotted in Fig. 2(a). At all temperatures, $R(\omega)$ increases monotonically with decreasing frequency but shows a broad hump above 2000 cm^{-1} . Below 200 cm^{-1} , as compared in the inset of Fig. 2(a), $R(\omega)$ at 6 K increases faster towards unity (at zero frequency) than those of 60 K. Consequently, one sees a small frequency edge that indicates a gap partially opening at low temperatures. These features are more pronounced in the real part of the optical conductivity $\sigma_1(\omega)$ shown in Fig. 2(b). Above 40 K, the spectrum is characteristic of a broad Drude-like peak in the low-frequency region and an almost T -independent interband transition peak at high frequencies. Below 10 K, the broad Drude peak starts to be suppressed, revealing a potential narrower Drude peak below 150 cm^{-1} and a Lorentz-like peak around 400 cm^{-1} . Limited by our low-frequency reflectivity measurement, only a tail of this low-temperature Drude peak could be seen in Fig. 2(b). However, the development of the gap structure and the Lorentz peak is evident, consistent with the expectation of a hybridization gap opening above the flat heavy electron band around the Fermi energy in typical heavy fermion compounds.

By contrast, the above gap feature is absent in the perpendicular direction. Figure 3(a) plots the reflectivity spectra $R(\omega)$ with $E \perp c$. The corresponding optical spectra are shown in Fig. 3(b). We see a broad Drude-like peak from 300 to 6 K but no gap feature appears over the whole frequency range down to 80 cm^{-1} . On the other hand, $\sigma_1(\omega)$ at very low frequencies around 80 cm^{-1} does seem to decrease slightly with decreasing temperature below 40 K, consistent with the negative T dependency of the resistivity plotted in Fig. 1(a). Thus there is no sign of a gap opening perpendicular to the c axis within our measured temperature and frequency range. The increase of the resistivity with lowering temperature suggests an even enhanced spin scattering from 50 K all the way down to the lowest measured temperature 2 K. We hence conclude that the hybridization gap only opens along the c axis and is highly anisotropic in the momentum space [15]. It has a magnitude of roughly 368 cm^{-1} or 46 meV at 6 K estimated from the position of the midinfrared Lorentz-like peak.

The above observation along the c axis is similar to that reported in many heavy fermion compounds [16], where the opening of the hybridization gap reflects the emergence of itinerant heavy electrons below the coherence temperature T^* . At high temperatures, the f electrons are well localized, so the

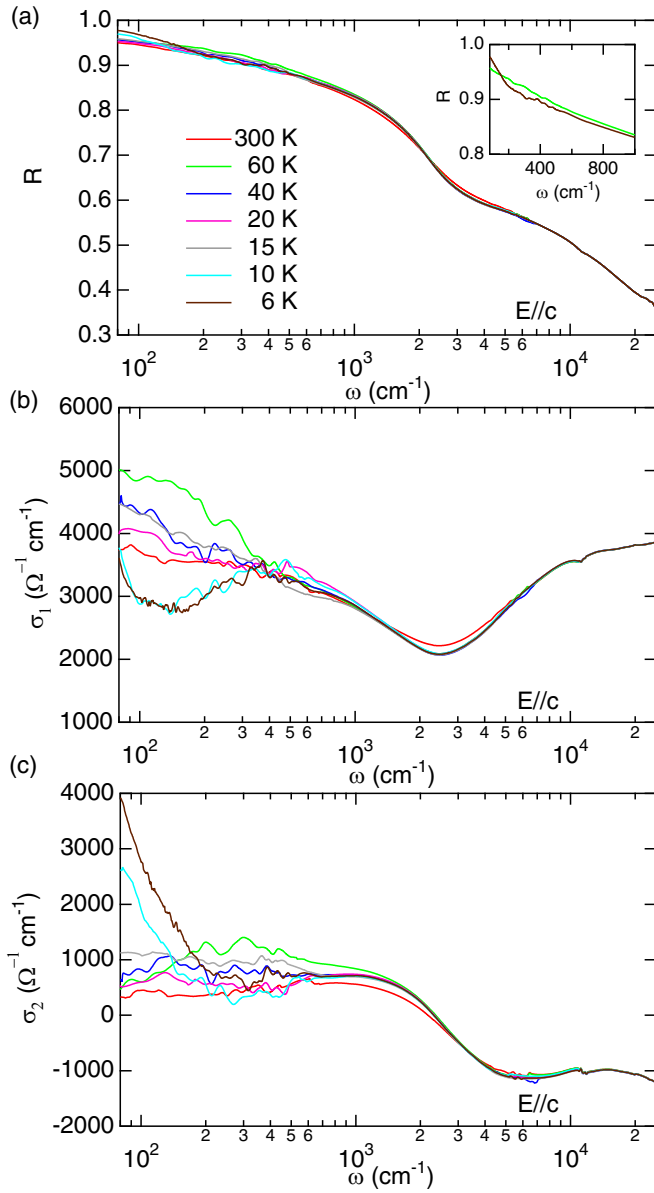


FIG. 2. Frequency dependence of (a) the reflectivity $R(\omega)$, (b) the real part of the optical conductivity $\sigma_1(\omega)$, and (c) the imaginary of the optical conductivity $\sigma_2(\omega)$, at different temperatures for $E \parallel c$. The inset of (a) compares the low- ω reflectivity spectra at 6 and 60 K in an enlarged scale.

conduction electrons give rise to the single broad Drude peak due to incoherent Kondo scattering by localized f moments. When the temperature is decreased across T^* , the f moments start to be partially screened due to spin entanglement with conduction electrons, forming two flat hybridization bands near the Fermi energy with a hybridization gap in between. As a result, the single broad Drude peak splits into a narrower Drude peak representing the intraband transition of coherent heavy electrons and a Lorentz peak originating from a direct interband transition across the hybridization gap.

To gain more insight into the charge dynamics of the correlated state below T^* , we apply the extended Drude

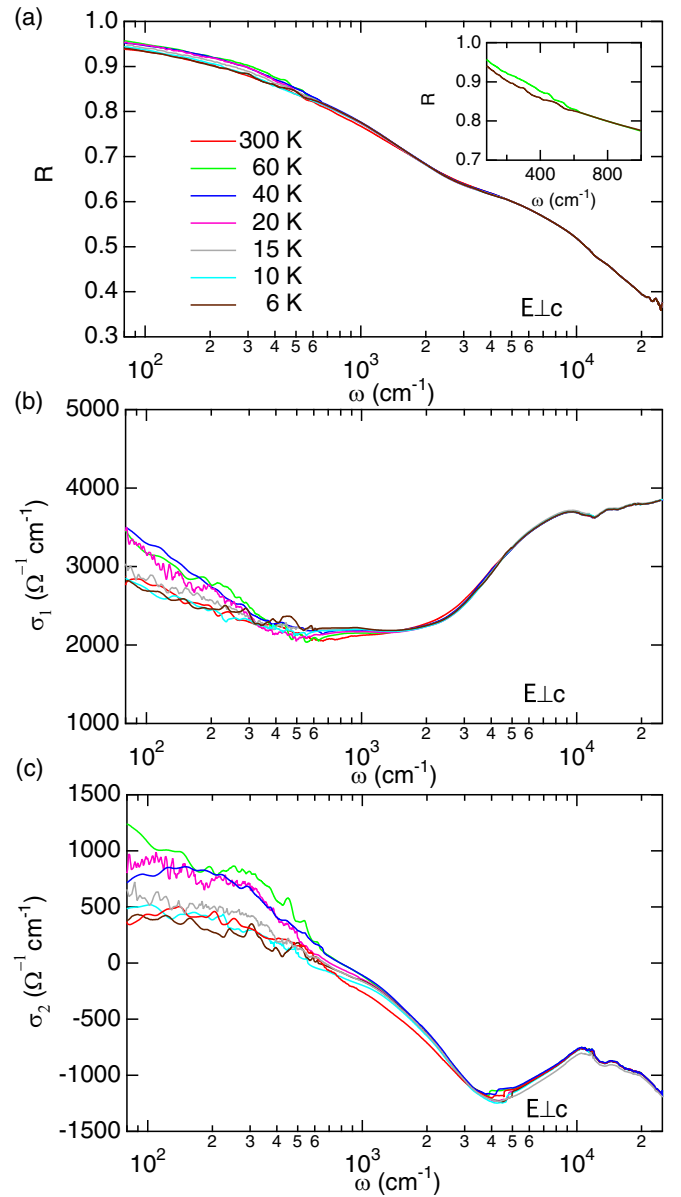


FIG. 3. Frequency dependence of (a) the reflectivity $R(\omega)$, (b) the real part of the optical conductivity $\sigma_1(\omega)$, and (c) the imaginary of the optical conductivity $\sigma_2(\omega)$, at different temperatures for $E \perp c$. The inset of (a) compares the low- ω reflectivity spectra at 6 and 60 K in an enlarged scale.

model [17,18],

$$\sigma(\omega) = \frac{\omega_p^2}{4\pi} \frac{1}{1/\tau(\omega) - i\omega m^*(\omega)/m_b}, \quad (1)$$

where $\tau(\omega)$ and $m^*(\omega)$ are the frequency-dependent lifetime and effective mass, respectively. One may then derive from the experimental data,

$$\begin{aligned} 1/\tau(\omega) &= \omega_p^2 \sigma_1(\omega) / 4\pi |\sigma(\omega)|^2, \\ m^*(\omega)/m_b &= \omega_p^2 \sigma_2(\omega) / 4\pi \omega |\sigma(\omega)|^2, \end{aligned} \quad (2)$$

where $\sigma_1(\omega)$ and $\sigma_2(\omega)$ are the real and imaginary parts of the optical conductivity, respectively, and m_b is the band mass. The plasma frequency $\omega_p^2 = 4\pi e^2 n / m_b$ is estimated by

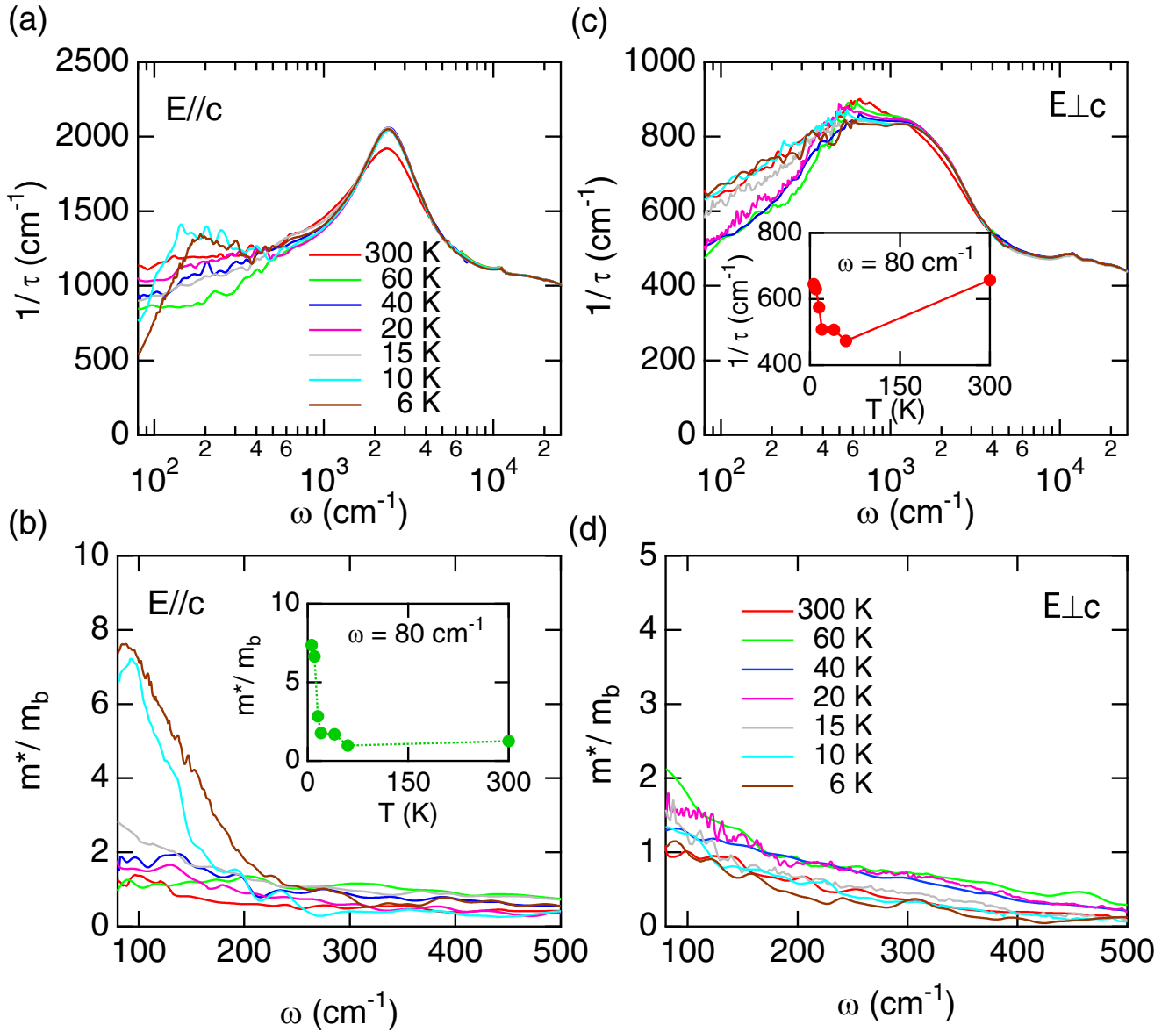


FIG. 4. Frequency dependence of the derived scattering rate $1/\tau(\omega)$ and the mass enhancement m^*/m_b at different temperatures for (a), (b) $E \parallel c$ and (c), (d) $E \perp c$. The inset of (b) plots the temperature dependence of the mass enhancement m^*/m_b at 80 cm^{-1} in the $E \parallel c$ direction. The inset of (c) shows the temperature dependence of $1/\tau(\omega)$ at 80 cm^{-1} in the $E \perp c$ direction.

integrating $\sigma_1(\omega)$ up to a cutoff frequency ω_c corresponding to the onset of intraband absorption [19], namely, $\omega_p^2/8 = \int_0^{\omega_c} \sigma_1(\omega) d\omega$. Here, for simplicity, we choose ω_c to be the minimum of $\sigma_1(\omega)$ at 300 K which is about 2550 cm^{-1} for $E \parallel c$ and 1400 cm^{-1} for $E \perp c$, corresponding to the fast drop in the reflectivity spectra at all temperatures. There is also a low-frequency cut at 80 cm^{-1} due to the limitation of our measurement, which introduces an additional uncertainty on the exact value of ω_p . However, these uncertainties do not affect our qualitative analysis of the overall frequency dependence of the scattering rate and effective mass.

Figure 4 plot the resulting $1/\tau(\omega)$ and $m^*(\omega)$ for the two field directions, respectively. For $E \parallel c$, the two quantities are both weakly frequency dependent above 15 K. As the temperature is lowered across T^* down to 10 K, they start to show anomalous variations below 300 cm^{-1} . At 10 and 6 K,

a sharp peak appears at around 200 cm^{-1} in $1/\tau(\omega)$. Since this frequency corresponds to the range of the hybridization gap, the maximum in $1/\tau(\omega)$ indicates that the charge carriers are strongly damped due to the coupling to hybridization fluctuations. In other words, the excited heavy quasiparticles may decay into the conduction electrons and f moments that they are made of. At lower frequencies, $1/\tau(\omega)$ drops rapidly, marking the onset of coherence at lower energies. The fact that $1/\tau(\omega)$ becomes even smaller than its high-temperature values indicates the weakening of incoherent scattering due to heavy electron formation. Correspondingly, the effective mass $m^*(\omega)/m_b$ also increases with lowering frequency. The temperature dependence of $m^*(\omega)/m_b$ at 80 cm^{-1} is displayed in the inset of Fig. 4(b). We see a rapid increase of the mass enhancement over 6 below 10 K. One may have noticed that this mass enhancement is still not as high as that estimated from

the specific heat coefficient, which is about 400 mJ/mol K² at 6 K compared to 8.4 mJ/mol K² for LaCo₂Ga₈ [8]. This is expected because our estimate is obtained at a finite frequency of 80 cm⁻¹ and an exact comparison to the thermodynamic mass enhancement is only appropriate in the zero-frequency limit, given the rapid increase of $m^*(\omega)$ with lowering frequency. A similar underestimation by optical measurement has been seen previously also in other heavy fermion compounds such as CeCoIn₅ [20,21].

By contrast, no such anomalous behavior can be observed along the perpendicular direction. As shown in Figs. 4(c) and 4(d), both $1/\tau(\omega)$ and $m^*(\omega)$ remain featureless at low frequencies for all temperatures, suggesting the absence of a gap opening perpendicular to the c axis within our measured temperature and frequency range. The temperature dependence of the scattering rate $1/\tau(\omega)$ at 80 cm⁻¹ is plotted in the inset of Fig. 4(c). The nonmonotonic behavior agrees well with the dc resistivity, confirming the increased behavior of the resistivity with lowering temperature in the perpendicular direction owing to the enhanced spin scattering at low temperatures.

Thus, our experiment establishes the uniaxial hybridization and quasi-1D nature of the emergent heavy electron state in a single crystal of CeCo₂Ga₈ and confirms the correspondence between the microscopic charge dynamics and the macroscopic transport properties. Previously, it has been noticed that in many heavy fermion compounds the coherence temperature T^* is anisotropic [22]. The nature of this anisotropy remains to be clarified [23,24]. Our observation in CeCo₂Ga₈ pushes this to an extreme situation where coherence only occurs along a single direction and the perpendicular directions remain incoherent, despite that at high temperatures or high frequencies

the conduction electron background shows less anisotropy along different directions. This suggests that the coherence temperature is not a local quantity purely determined by the Kondo screening energy scale. Rather, it is closely associated with the lattice properties reflecting a certain intersite correlation effect between localized f moments [22,25]. This may have a deep implication on our understanding of heavy fermion physics.

To summarize, we report the reflectivity and optical spectra measurements of CeCo₂Ga₈ using polarized light along and perpendicular to the c axis. Our results reveal a strong anisotropy at low frequencies and low temperatures. When the temperature is lowered across the coherence temperature, the low-frequency spectra along the c axis are found to split into a narrow Drude peak below 100 cm⁻¹ and a midinfrared peak around about 400 cm⁻¹, manifesting the opening of a hybridization gap in typical heavy fermion metals. However, the splitting is absent in the perpendicular direction, thus confirming the quasi-1D nature of the heavy electron state. CeCo₂Ga₈ is therefore a rare example of the quasi-1D Kondo lattice and may be a useful platform for studying the heavy fermion physics at low dimensionality.

This work was supported by the National Key R&D Program of China (Grants No. 2018YFA0305702, No. 2017YFA0303103, and No. 2016YFA0300303), the National Natural Science Foundation of China (NSFC Grants No. 11774401, No. 11974397, and No. U2032204), the Strategic Priority Research Program of the Chinese Academy of Sciences (Grant No. XDB33010100), and the K. C. Wong Education Foundation (GJTD-2018-01).

P.Z. and C.W. contributed equally to this work.

-
- [1] H. Okamura, T. Michizawa, T. Nanba, and T. Ebihara, *J. Phys. Soc. Jpn.* **73**, 2045 (2004).
- [2] S. Kimura, J. Sichelschmidt, J. Ferstl, C. Krellner, C. Geibel, and F. Steglich, *Phys. Rev. B* **74**, 132408 (2006).
- [3] V. A. Sidorov, M. Nicklas, P. G. Pagliuso, J. L. Sarrao, Y. Bang, A. V. Balatsky, and J. D. Thompson, *Phys. Rev. Lett.* **89**, 157004 (2002).
- [4] T. Kasuya, *Europhys. Lett.* **26**, 277 (1994).
- [5] S. -i. Kimura, T. Iizuka, H. Miyazaki, A. Irizawa, Y. Muro, and T. Takabatake, *Phys. Rev. Lett.* **106**, 056404 (2011).
- [6] Y.-F. Yang and D. Pines, *Phys. Rev. Lett.* **100**, 096404 (2008).
- [7] J. H. Shim, K. Haule, and G. Kotliar, *Science* **318**, 1615 (2007).
- [8] L. Wang, Zh. M. Fu, J. P. Sun, M. Liu, W. Yi, Ch. J. Yi, Y. K. Luo, Y. M. Dai, G. T. Liu, Y. Matsushita, K. Yamaura, L. Lu, J. G. Cheng, Y.-F. Yang, Y. G. Shi, and J. L. Luo, *npj Quantum Mater.* **2**, 36 (2017).
- [9] K. Q. Cheng, L. Wang, Y. J. Xu, F. Yang, H. P. Zhu, J. Z. Ke, X. F. Lu, Z. C. Xia, J. F. Wang, Y. G. Shi, Y. F. Yang, and Y. K. Luo, *Phys. Rev. Mater.* **3**, 021402(R) (2019).
- [10] F. Steglich, H. Pfau, S. Lausberg, S. Hamann, P. Sun, U. Stockert, M. Brando, S. Friedemann, C. Krellner, C. Geibel, S. Wirth, S. Kirchner, E. Abrahams, and Q. Si, *J. Phys. Soc. Jpn.* **83**, 061001 (2014).
- [11] P. Wölfle and E. Abrahams, *Ann. Phys. (Berlin)* **523**, 591 (2011).
- [12] A. Steppke, R. Küchler, S. Lausberg, E. Lengyel, L. Steinke, R. Borth, T. Lühmann, C. Krellner, M. Nicklas, C. Geibel, F. Steglich, and M. Brando, *Science* **339**, 933 (2013).
- [13] B. Shen, Y. Zhang, Y. Komijani, M. Nicklas, R. Borth, A. Wang, Y. Chen, Z. Nie, R. Li, X. Lu, H. Lee, M. Smidman, F. Steglich, P. Coleman, and H. Yuan, *Nature (London)* **579**, 51 (2020).
- [14] W. Z. Hu, J. Dong, G. Li, Z. Li, P. Zheng, G. F. Chen, J. L. Luo, and N. L. Wang, *Phys. Rev. Lett.* **101**, 257005 (2008).
- [15] K. S. Burch, S. V. Dordevic, F. P. Mena, A. B. Kuzmenko, D. van der Marel, J. L. Sarrao, J. R. Jeffries, E. D. Bauer, M. B. Maple, and D. N. Basov, *Phys. Rev. B* **75**, 054523 (2007).
- [16] S. V. Dordevic, D. N. Basov, N. R. Dilley, E. D. Bauer, and M. B. Maple, *Phys. Rev. Lett.* **86**, 684 (2001).
- [17] J. W. Allen and J. C. Mikkelsen, *Phys. Rev. B* **15**, 2952 (1977).
- [18] F. P. Mena, D. van der Marel, and J. L. Sarrao, *Phys. Rev. B* **72**, 045119 (2005).
- [19] M. K. Stewart, D. Brownstead, S. Wang, K. G. West, J. G. Ramirez, M. M. Qazilbash, N. B. Perkins, I. K. Schuller, and D. N. Basov, *Phys. Rev. B* **85**, 205113 (2012).

- [20] E. J. Singley, D. N. Basov, E. D. Bauer, and M. B. Maple, *Phys. Rev. B* **65**, 161101(R) (2002).
- [21] C. Petrovic, P. G. Pagliuso, M. F. Hundley, R. Movshovich, J. L. Sarrao, J. D. Thompson, Z. Fisk, and P. Monthoux, *J. Phys.: Condens. Matter* **13**, L337 (2001).
- [22] Y.-F. Yang, Z. Fisk, H.-O. Lee, J. D. Thompson, and D. Pines, *Nature (London)* **454**, 611 (2008).
- [23] K. Ohishi, R. H. Heffner, T. U. Ito, W. Higemoto, G. D. Morris, N. Hur, E. D. Bauer, J. L. Sarrao, J. D. Thompson, D. E. MacLaughlin, and L. Shu, *Phys. Rev. B* **80**, 125104 (2009).
- [24] Y.-F. Yang, *Rep. Prog. Phys.* **79**, 074501 (2016).
- [25] S. Nakatsuji, S. Yeo, L. Balicas, Z. Fisk, P. Schlottmann, P. G. Pagliuso, N. O. Moreno, J. L. Sarrao, and J. D. Thompson, *Phys. Rev. Lett.* **89**, 106402 (2002).